

A novel AI-AVO approach for maximum power generation of PMSG

Prashant Kumar S. Chinamalli, Mungamuri Sasikala

Department of Electrical and Electronics Engineering, Shambasva University, Kalaburagi, India

Article Info

Article history:

Received Dec 18, 2023

Revised Jun 8, 2024

Accepted Jun 25, 2024

Keywords:

IPMSG

Optimization

PMSGs

Tip speed ratio

Wind power generation

ABSTRACT

Permanent magnet synchronous generators (PMSGs) are necessary for producing wind energy that is both highly reliable and reasonably priced. An inventive control technique for the driven interior PMSG (IPMSG) is presented here to maximize wind energy output and decrease losses. This research established an innovative optimization strategy for the highest wind power generation with reduced overall loss in PMSG-based Wind power generation systems. Considering, that the tip speed ratio (TPR), rotor speed ω_r , and quadrature axis current I_q are optimized in the proposed work in such a way to enhance wind power generation. Further, the direct axis current I_d is calculated from the optimized rotor speed ω_r . The minimization of core loss is considered as the fitness function, which is a function of the direct current axis I_d and quadrature current axis I_q . The optimization is carried out using the explored aquila with African vulture optimization (EA-AVO) technique, which is the conceptual incorporation of prevailing techniques, like the aquila optimization algorithm (AOA) and the AVO algorithm. The performance of the proposed method is validated over the conventional methods, in terms of power output, losses, efficiency, and convergence analysis. According, the findings show that the proposed method attains less overall loss of 149.62 at the starting stage of 50 rotor speed, and it was 36.46% higher than AQO, 36.17% higher than AVOA, 36.59% higher than GOA methods 36.42%, and higher than WHO+PI approaches.

This is an open access article under the [CC BY-SA](#) license.



Corresponding Author:

Prashant Kumar S. Chinamalli

Department of Electrical and Electronics Engineering, Sharnbasva University

Kalaburagi, India

Email: prashantvneec@gmail.com

1. INTRODUCTION

Wind energy, a renewable form of electrical energy, can be viewed as offering a supportable energy source. Moreover, its potential for commercial success is beneficial to the world. It has become vital to create grid integration along with the usage of inverters to control frequency, and reactive/active power, and to provide grid voltage support as the use of renewable energy sources increases [1], [2]. Grid-connected and stand-alone wind energy conversion systems (WECS) have both been subjected to control strategies [3], [4]. In addition, grid operators need to make sure that both active and reactive powers are supplied to the system [5], [6]. Squirrel-cage induction generators, permanent magnet synchronous generators (PMSGs), doubly-fed induction generators (DFIGs), high-temperature superconducting synchronous generators (HTS-SGs), and wound rotor synchronous generators are among the different types of generators used by WECS. In recent years, PMSMs have been attracted for their usage in the production of wind energy [7]-[9]. Therefore, in rotor circuits, there is no need for external resistance and copper losses, such that the PMSMs can produce

power with excellent efficiency. Because of its compact size and excellent power density, wind turbines may be built more affordably and with less weight. Owing to their outstanding performance, great dependability, and low cost, PMSMs are commonly employed in tiny variable-speed wind turbines. Copper, core and stray-load losses were minimized when designing the control system for the IPMSM as mentioned in [10]. However, the IPMSM's operational limits and saturation effect were not taken into account by the authors. Thus, the stator copper and core losses of the IPMSM were reduced [11] by using an online iterative search technique. Therefore, a time-consuming analysis is also produced by the online search for the ideal value which lowers the total efficiency of the control system. Designing high-performance nonlinear current controllers using the input-output feedback linearization (IOL) approach eliminates the consequences of nonlinearity brought on by magnetic saturation [12]. The suggested controlling approach enhances the dynamic effectiveness of the wind-generating system [13]-[15].

Compared to other PMSMs, IPMSMs can use flux weakening along the d-axis to keep a consistent power over a wide range of speeds and can generate power with maximum effectiveness and excellent controllability using reluctance torque about magnetic torque [16], [17]. Yet, the IPMSM's q-axis inductance changes in contrast to the q-axis stator current which may cause a magnetic saturation effect. Furthermore, the produced torque in an IPMSM is influenced by the two separate d-q-axis stator current components. If the d-axis stator-current component is present in the flux-weakening zone, where the IPMSM operates, then, the system linearity consequently worsens [18], [19]. Therefore, the direct application of sophisticated linear-system theory is complicated by this nonlinearity. To address this issue and enhance the functionality of IPMSMs, nonlinear control techniques have been established [20]. Further, an efficient maximum power point tracking (MPPT) technique is necessary for modern conversion systems to develop the energy capture effectiveness from wind and also to reduce the losses. This study investigated the effects of a novel control scheme for an IPMSG. While earlier studies have explored the impact of losses in driven Interior PMSG, they have not explicitly addressed its influence on PMSG-based wind power generation systems.

The contributions of this research are discussed:

- Design a novel control scheme for an IPMSG, in which the polynomial restrictions are handled optimally to maximize wind energy output by minimizing IPMSG losses.
- Propose a new hybrid model known as explored aquila with African vulture optimization (EA-AVO) Algorithm that hybridises the concepts of AOA and AVOA.
- The optimal solution of AOA is given as an input to AVOA, in which the best solution is attained to optimally tune the tip speed ratio (TPR), rotor speed and quadrature axis current to enhance wind power generation.

The study is organized as follows: section 2 deliberates the literature work. Section 3 describes the maximum wind turbine generation of the IPM synchronous generator. Section 4 describes the optimization of optimal current I_q using the hybrid EA-AVO approach, section 5 deliberates the attained outcomes and section 6 concludes the paper.

2. LITERATURE REVIEW

2.1. Related works

In 2018, Chinamalli and Sasikala [21] developed an innovative control framework for the internal PMSG-driven model, which demonstrates how the polynomial parameters are most effective in achieving the peak or maximal wind power generation and minimising the loss of IPMSG. This study suggests a novel hybridised method called CWOA, which selects its coefficients for effective power generation. Additionally, as the TPR is a crucial factor in the production of wind energy, it is also optimally set. The control scheme architecture takes responsibility for the influence of magnetic saturation, which results in the extremely nonlinear properties of the IPMSG. Thus, the suggestive CWOA's performance is measured in comparison to that of several well-known models, including the FF, GA, WOA, and ABC based on copper loss, core loss, and total loss.

In 2022, Mahmoud [22] presented an innovative WHO approach that was employed to design an ideal controller for a WTS using PMSG. The machine-side converter is controlled by a method that consists of two current loops of the optimized controller. The appropriate optimization of the PI controller improves the entire system response variables, thus the dynamic concern of PMSG may be enhanced under various conditions. This improvement thereafter enables the identification of the maximum power tracking during variations in wind speed and the fault ride-through capabilities during faults and large-signal occurrences. The analysis was performed in MATLAB simulations and evaluated the viability and efficacy of the suggested controller.

In 2021, Shanmugam and Joo [23] were concerned with the equilibrium study for a nonlinear wind turbine system using aPMSG under a FBMSD control scheme. According to this context, the offered nonlinear scheme is converted into linear-sub models using the T-S fuzzy theory and the appropriate FBMSD controller is established. The article offers an appropriate Lyapunov-Krasovskii functional that includes details on the sampling interval's length and a fixed transmission delay. Sufficient criteria have been determined in the form of linear matrix inequalities to maintain the suggested structure. The outcome of the T-S fuzzy PMSG model is assessed using certain data set values as a test benchmark, and the result is then verified using derived conditions. In conclusion, it was shown that the suggested FBMSD controller guaranteed the sturdiness performance of PMSG based on WTS and was supported by numerical simulations.

In 2020, Dursun *et al.* [24] created an integrated structure that is beneficial to maximize the extraction of wind energy. Two hybrid MPPT techniques that combine CDW-PSO and GM-CPSO approaches are included in this structure, along with a fast terminal sliding mode-based MPPT controller. The highest possible value of the maximum energy to be collected was searched using CDW-PSO and GM-CPSO to identify the ideal parameters. These parameters must be selected in an ideal manner to produce the greatest power to guarantee MPPT efficiency. In contrast, the suggested hybrid MPPT approach is combined with FTSMC to bring the system to its optimal operating position. To emphasize the favourable characteristics of the suggested MPPT approaches, three specific wind speed situations are developed in a simulated environment. Thus, the suggested CDW-PSO-based ORB and GMC-PSO-based ORB MPPT methods are contrasted with standard ORB and TSR approaches about maximum generating power and MPPT efficiencies. The results of this research show that the offered optimization integrated approach increases MPPT efficacy and produces more wind energy compared with standard approaches.

In 2022, Hussien *et al.* [25] have suggested an MFO approach that helps to optimize the double controller that is employed with the PMSG on WECS. Using moth flame optimization, the WECS controller constraints are optimized to increase the amount of power sent to the grid. Moreover, GSC and generator MSC are utilized to create a grid-connected WECS with a PMSG. While the generator side converter was managed to increase power extraction, the grid side converter was optimized for power quality. Consequently, the resulting controller coefficients reduce overshoot and error at the steady-state level. In 2021, Fathy *et al.* [26] introduced an innovative and effective AOA technique for modelling MPPT fitted with the WECS. The system comprises a WT that is connected to a PMSG, a 3-phase rectifier that converts the generator's AC electrical output to DC, and a boost converter that accepts DC voltage as an input and regulates the MOSFET duty cycle. When addressing the intended power that is generated from the system, the entire design procedure is considered as an optimization issue. The suggested AOA adjusts the converter duty cycle to increase output power. This study follows three different scenarios: a fixed wind speed, a variable wind speed, and the actual wind speed as measured at four different locations in Saudi Arabia. To achieve the highest performance of the WECS, the findings proved the robustness of the suggested AOA-MPPT.

In 2020, Mahmoud and Abdel-Rahim [27] introduced different operating conditions to get the optimal parameters of the PI controller. The suggested PI-based WOA offers MPPT for variations in wind speed and also brings about a better understanding of the FRT potential. With a specific wind speed, the TSR technique is found successful in running PMSG at MPPT. BC was added to the DC circuit to assist PMSG in navigating grid faults. GWO outperforms different methods of optimization for PMSG when confronted with identical conditions of operation. The findings demonstrate that the GWO approach outperforms the WOA in terms of accomplishing FRT. At last, it can be said that in all of the situations examined, PMSG's functioning with the GWO approach according to PI controller and BC was the most successful.

In 2009, Qiao *et al.* [28] developed an innovative control strategy for a wind turbine-driven interior, in which the d-axis and q-axis stator-current features are effectively managed to accomplish the highest energy output and minimize the loss of the IPMSG. The control-scheme design incorporates the magnetic saturation's impact, which results in the IPMSG's extremely nonlinear properties. By resolving a restricted nonlinear optimization issue that reduces the IPMSG's copper as well as core losses, it is possible to determine the ideal d-axis stator-current command as a result of the IPMSG rotor speed. IOL approach is used to create high-performance nonlinear current controllers, which eliminates the impacts of nonlinearity brought on by magnetic saturation. The suggested control plan gives the optimal efficacy and higher dynamic performance of the generated wind system.

2.2. Review

Table 1 depicts the methods used for various systems built on IPMSG wind production. At first, the CWOA approach was suggested in [21] which offers maximal wind power and decreases the copper and core losses. However, tracking control does not function properly. Moreover, the WHO+PI strategy was implemented in [22], which provides a feasible solution and is highly effective. Nevertheless, DC voltage is severely impacted and worsens if MSC is unable to detect the malfunction. Furthermore, the FBMSD

controller was projected in [23] that ensure stability performance, but it has to focus more on nonlinear dynamical system stabilization problems. Similarly, CDW-PSO and GM-CPSO strategy was presented in [24], which deliver high energy and provide high MPPT efficacy. However, it needs to concentrate more on various controller design techniques and on optimizing the controller's attributes. Additionally, the MFO scheme was suggested in [25] that maximizes grid power and decreases both overshoot and steady-state error; anyhow, it converges unexpectedly, low population divergence and trapping of local optima are some of the drawbacks. Similarly, the AOA technique was developed in [26], which offers robustness and provide maximal power. However, a substantial challenge enhances the performance of the wind power-producing system, particularly when it operates in changeable weather circumstances. Furthermore, an optimization approach was suggested in [27] that offers highly superior performance with minimum cost, but it has a major disadvantage of complex structure and high oscillations. Finally, the IOL technique was implemented in [28] that offers better performance and their corresponding efficacy was high, but it can be challenging to directly apply the sophisticated linear-system theory. The aforementioned difficulties are taken into account as a motivation for improving wind turbine performance in IPMSG.

Table 1. Features and challenges of wind power generation from IPMSG based on various techniques

Author [citation]	Methodology utilized	Features	Challenges
Chinamalli and Sasikala [21]	CWOA approach	<ul style="list-style-type: none"> – Generate maximal wind power – Minimize the losses 	<ul style="list-style-type: none"> – Tracking control does not function properly.
Mahmoud [22]	WHO+PI strategy	<ul style="list-style-type: none"> – High effectiveness – Provide a feasible solution 	<ul style="list-style-type: none"> – DC voltage is severely impacted & worsened if MSC is unable to detect the malfunction.
Shanmugam and Joo [23]	FBMSD controller	<ul style="list-style-type: none"> – Ensure stable performance 	<ul style="list-style-type: none"> – Need to focus on nonlinear dynamical system stabilization problem
Dursun <i>et al.</i> [24]	CDW-PSO and GM-CPSO strategy	<ul style="list-style-type: none"> – Deliver high energy – Provide maximum MPPT efficacy 	<ul style="list-style-type: none"> – Need to concentrate on various controller design techniques and on optimizing the controller's attributes.
Hussien <i>et al.</i> [25]	MFO scheme	<ul style="list-style-type: none"> – Maximize grid power – Minimize both overshoot and steady-state error 	<ul style="list-style-type: none"> – Converges unexpectedly – Population divergence will be low. – Trapping into local optima.
Fathy <i>et al.</i> [26]	AOA technique	<ul style="list-style-type: none"> – maximal power – more robust 	<ul style="list-style-type: none"> – A substantial issue is increasing the performance of the wind power producing system, particularly when it operates in changeable weather.
Mahmoud [27]	Optimization strategies	<ul style="list-style-type: none"> – Highly superior – Cost is low 	<ul style="list-style-type: none"> – It has a major disadvantage of complex structure and high oscillations.
Qiao <i>et al.</i> [28]	IOL technique	<ul style="list-style-type: none"> – Efficacy is high – Better performance 	<ul style="list-style-type: none"> – It can be challenging to directly apply the sophisticated linear-system theory.

2.3. Research question

The following questions are the focus of this paper:

- Whether an effective MPPT technique is required to increase the effectiveness of wind energy capture and decrease losses?
- Does TPR, rotor speed and quadrature axis current affect the performance of the wind power generation. The objective function is defined based on the aforesaid research question.

3. MAXIMUM WIND POWER GENERATION FROM IPM SYNCHRONOUS GENERATOR

The IPMSG transforms the wind turbine's mechanical power into AC electrical power, which is subsequently transformed into DC electrical energy using an IGBT-based PWM converter linked by a DC connection for supplying the DC load. By altering the electrical voltages on the AC side of the PWM power converter, the IPMSG may be controlled. The IPMSG can provide AC electrical energy to the power grid or an AC load with a constant voltage and frequency by using an extra energy inverter. Moreover, the wind turbine extracts mechanical power from the wind, which is determined using (1).

$$P_M = \frac{1}{2} \rho A_{rb} V_w^3 P_{coef}(\lambda, \beta) \quad (1)$$

Where ρ specifies the thickness of air (kilograms/cubic meter), the area of the rotor blades (m^2) is given as $A_{rb} = \pi R_{wt}^2$ and R_{wt} is the radius of the rotor in metre, V_w defines the speediness of the wind in metres per second, and P_{coef} is the power factor with tip-speed ratio λ and blade pitch angle β and is given in [29].

$$P_{coef} = 0.5(\lambda - 0.022\beta^2 - 5.6)e^{-0.17\lambda} \tag{2}$$

Where λ is determined by $N_r R_{wt}/V_w$ and N_r defines the wind turbine rotation speed (rad/sec).

3.1. System model of IPMSG

Figure 1 depicts the proposed model of the IPMSG system which comprises the effect of the stator core and copper losses. Equivalent core-loss resistance R_{cl} is employed to symbolize the core loss, which is brought on by hysteresis and eddy currents. Moreover, a technique is offered to ascertain the value of R_{cl} which is a linear function of IPMSG rotor speed ω_r as represented in [30].

$$R_{cl} = k_r \omega_r \tag{3}$$

Where, $k_r = 0.2083$ (ohm/rpm).

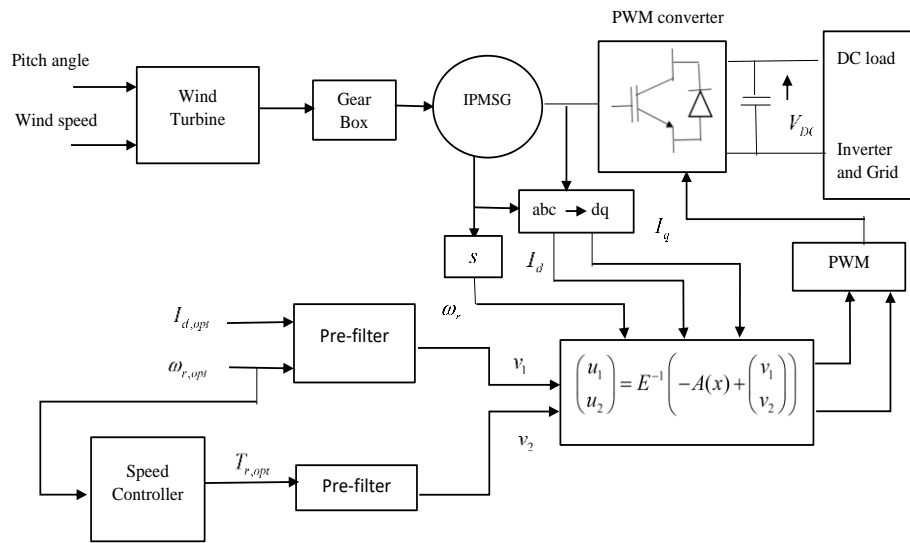


Figure 1. System model of IPMSG

The rotor magnetic circuit becomes more salient for the IPMSG when the magnets are buried into the rotor. A large area of magnets with poor penetrability is traversed by the d-axis flux, but the q-axis flux route exhibits a high penetrability. Due to the salient nature of the IPMSG ($L_q > L_d$), the q-axis with magnetic saturation is a dominating phenomenon. Whenever this saturation is included, the dynamical model of a three-phase IPMSG can be expressed in the reference frame of the rotor as,

$$L_d \frac{dI_{d0}}{dt} = -R_{stator}I_d + \omega L_q(I_q)I_{q0} + V_d \tag{4}$$

$$L_q(I_q) \frac{dI_{q0}}{dt} = -R_{stator}I_q + \omega L_d I_{d0} - \omega \phi_r + V_q \tag{5}$$

where, ϕ_r denotes the magnetic flux linkage; R_{stator} is the resistance of the stator; L_d and L_q signifies the inductance of the d-q axis in which L_q varies liable on the I_q value as mentioned in [31]-[33]. However, by modelling L_q as a function of I_q as indicated by (6), allows one to consider the impact of magnetic saturation.

$$L_q = L_{q1} - K|I_q| \tag{6}$$

Where, K is a constant value with a positive integer. Furthermore, the incorporation of magnetic saturation in the framework makes it difficult to directly apply linear-system theory and loss-minimization techniques to the IPMSG; therefore, here, this problem is tackled in a nonlinear manner. The electrical torque T_E developed in IPMSG is:

$$T_E = -\frac{3}{4}P_N \left[\varphi_r I_{qo} + (L_d - L_q(I_q)) I_{do} I_{qo} \right] \quad (7)$$

3.2. Optimum stator q-axis current control

The optimum I_q value is determined using the electrical torque as defined in (7). The overall core and copper losses L_{total} of the IPMSG serve as the fitness function. The first two constraint equations can be evaluated, by addressing the problems with irregular optimization for various IPMSG rotor speeds, the optimum value I_q can be attained. To estimate the correlation between the ideal d-q-axis stator current constituents and the IPMSG rotor speed, the below equations are used:

$$I_{q,opt} = k_{q3}\omega_r^3 + k_{q2}\omega_r^2 + k_{q1}\omega_r + k_{q0} \quad (8)$$

The coefficients as noted in (8) only offer the IPMSG's ideal operating parameters that exceed the wind speed rather than the operating values. Thus, the terminal voltage as well as phase current reaches their upper limit levels by preventing the best speed tracking control. In this circumstance, the IPMSG can be controlled to obtain the highest possible output.

4. OPTIMIZATION OF OPTIMAL CURRENT I_Q USING HYBRID EA-AVO APPROACH

4.1. Maximal wind energy production

The wind turbine shaft rotation speed is properly measured so that the TPR λ is sustained at the desired value to attain the most significant energy coefficient without considering the wind speed. As a result, wind energy is used to generate high mechanical energy. The optimum rotor speed of IPMSG as stated in (1) is directly related to wind speed while k_{wt} representing an unchanged value which can be determined by the wind turbine constraints.

$$\omega_{r,optimal} = k_{wt}V_w \quad (9)$$

4.2. Objective function for reducing core and copper losses

The four primary aspects of the PMSG losses are mechanical loss, stator copper loss, stray-load loss and core losses. Furthermore, the fundamental aspects of stator currents may be used to regulate core losses as well as the copper losses in the stator, which are entirely dependent on each other. Thus, the system achieves increased IPMSG efficiency with the limitations by overcoming the nonlinear optimization problems listed follows to decrease the IPMSG's core and copper losses:

$$\text{Minimization of } L_{Total} = L_{copper} + L_{core} \quad (10)$$

$$\text{Subject to } L_{copper} = 1.5R_{stator}(I_d^2 + I_q^2) \quad (11)$$

$$I_d = -V^{-1}(WI_{de}^2 + XI_{de}^3 + YI_{de}^4 - Z) \quad (12)$$

$$V = \varphi_r^3 \lambda + \omega^2 - 2I_q^2 \sigma^2 \varphi_r L_d^4 \alpha \lambda \omega^2 (R_{stator} + R_{cl}) \quad (13)$$

Where, $\varphi_r = 0.246$; $R_{stator} = 0.1764$, I_{de} = Sum of I_d signals, I_q be the optimal solution with a minimum bound of -50 and maximal bound of 10. The λ be the optimal solution with a minimum bound of 6 and a maximum bound of 30. R_{stator} and R_{cl} implies the resistance of the stator and core-loss:

$$R_{cl} = k_r * \omega_r = (0.2083/60) * (1200/60) \quad (14)$$

$$\omega = \frac{P_n * \omega_r}{2} = \frac{6 * (1200/60)}{2} \quad (15)$$

$$\sigma = \frac{L_q}{L_d} = \frac{20.5822 * 10^{-3}}{6.24 * 10^{-3}} \quad (16)$$

$$W = 3 \left((\omega^2 * L_d^2 * (R_{stator} + R_{cl}) * \varphi_r^2 * \alpha) + (1 + \alpha) * \left((L_d \varphi^2 \alpha \lambda) - \left((2 * I_q^2 * \sigma^2 * \varphi_r * L_d^5 * \alpha^3 * \lambda * \omega^2) (R_{stator} + R_{cl}) \right) \right) \right) \quad (17)$$

$$X = \left(\begin{array}{c} (3 * L_d^2 * \varphi_r * \alpha^2 * \lambda) + (3 * \omega^2 * L_d^4 * \alpha^2) \\ (R_{stator} * R_{cl}) * \varphi_r (1 + \alpha) \end{array} \right) \quad (18)$$

$$Y = (L_d^2 * \alpha^3 * \lambda) + (L_d^5 * \alpha^3 * \omega^2) (R_{stator} + R_{cl}) \quad (19)$$

$$Z = -(I_q^2 * \varphi_r^2 * \sigma^2 * L_d^3 * \lambda * \omega^2 * \alpha) \tag{20}$$

$$L_{core} = 1.5(I_{de}^2 + I_{qe}^2)R_{cl}(\omega_r) \tag{21}$$

$$L_{core} = 1.5\omega^2 [(L_d I_{do} + \varphi_r)^2 + (L_q(I_q)I_{qo})^2] / R_{cl}(\omega_r) \tag{22}$$

From (1)-(3), (6), and (7):

$$V_d = R_{stator}I_d - \omega L_d(I_q)I_{qo} \tag{23}$$

$$V_q = R_{stator}I_q + \omega L_d I_{do} + \omega \varphi_r \tag{24}$$

$$I_{do} = I_d - (V_d - R_{stator}I_d) / R_{cl}(\omega_r) \tag{25}$$

$$I_{qo} = I_q - (V_q - R_{stator}I_q) / R_{cl}(\omega_r) \tag{26}$$

$$T_M - T_E - D\omega_r = 0 \tag{27}$$

$$T_M = P_M / \omega_r \tag{28}$$

$$\omega = P_N \omega_r / 2 \tag{29}$$

$$I_d^2 + I_q^2 \leq I_{max}^2 \tag{30}$$

$$V_d^2 + V_q^2 \leq V_{max}^2 \tag{31}$$

While, L_{copper} and L_{core} signifies the copper and core loss. I_{max} and V_{max} denote the maximal current and voltage of IPMSG. This paper elaborates on an innovative optimization strategy for higher wind power generation with reduced overall loss in PMSG-based Wind energy production systems. Considering [21], the TPR, rotor speed ω_r and quadrature axis current I_q will be optimized in the proposed work in such a way to enhance wind power generation. Further, the direct axis current I_d will be calculated from the optimized rotor speed ω_r . The minimization of core loss is considered as the fitness function of I_d and I_q axis currents. To obtain the optimal solution, a hybrid optimization known as EA-AVO Algorithm is proposed.

4.3. Proposed EA-AVO approach

A new meta-heuristic method called AVOA was developed after analyzing the eating and orienting habits of African vultures [34]. Vultures are split into two groups depending on their physical abilities by how they behave in the wild. Additionally, vultures also spend hours seeking food due to their need to eat, which helps them escape the hunger trap. Further, two of the greatest solutions are regarded as the best and strongest vultures.

(i) Choosing the ideal vulture for each group

According to the fitness performance, both the primary and secondary vultures are chosen for global optimization in the initial phase of the AVOA methodology. The subsequent formulae indicate the option of selecting the vultures.

$$H(i) = \begin{cases} \text{Bestvulture}_1 & \text{if } q_i = \delta \\ \text{Bestvulture}_2 & \text{if } q_i = \lambda \end{cases} \tag{32}$$

In (32), the quantitative variables, such as δ and λ are fixed before the searching procedure. Each of these variables has a value that ranges from 0 to 1, and the overall significance of the two parameters is equal to 1. A roulette wheel can be used to select any of the finest options using (33).

$$q_i = \frac{S_i}{\sum_{i=1}^n S_i} \tag{33}$$

If δ is very near to one, exploitation may increase. In (34) provides a mathematical formulation for the vulture vigour rate, which is determined by vulture behaviour, a shortage of energy and aggressive behaviour while seeking food.

$$S = (2 \times r_1 + 1) \times y_i \times \left(1 - \frac{it}{it_{max}}\right) \quad (34)$$

The vulture's level of satiety is indicated by the variable S in (33) and it shows the present iteration count. it_{max} be the overall iteration count, and y_i is a randomized value among -1 and 1, which varies every time if it is repeated. The vulture is hungry if the value of y_i is less than 0; else, there are no vultures; r_1 is an arbitrary value that varies from 0 to 1. The equilibrium between exploring and exploiting is achieved in the AVOA technique by the value of the variable S . When the value $|S|$ exceeds 1, it moves into the exploring stage else moves to the exploiting stage.

(ii) Exploring stage

In this exploring stage, AO [16] is inherited into the AVOA, because AO has its major advantages, such as robustness and less overwhelmed by the population size. Moreover, the Aquila recognises the prey region and selects the ideal chasing zone by high-level soaring having an upright stoop. The AO investigates this area in depth while flying up to identify the search space's target region. Hence, it is known as the EA-AVO Algorithm.

$$q(i+1) = H(i) * \left(1 - \frac{it}{it_{max}}\right) \quad (35)$$

Whereas, $H(i)$ is the optimal vulture defined in eqn. (32); $q(i+1)$ defines the subsequent iteration's vulture location. X_m implies the mean value of the present iteration and is given by,

$$X_m = \frac{1}{n} \sum_{i=1}^n X_i \quad (36)$$

$$q(i+1) = H(i) - S + r_2 \times ((u_b - l_b) \times r_3 + l_b) \quad (37)$$

where, r_2 and r_3 define the randomized count amongst 0 and 1; u_b and l_b implies the top and bottom bounds.

(iii) Exploiting stage

During this stage of the AVOA algorithm, convergence and efficacy are defined. For this stage, two methods are modified by perceiving two parameters, q_2 and q_3 . These values range from 0 to 1. All the exploiting strategies are outlined here.

Stage 1:

In the initial stage, two alternative siege-fight and rotational flight techniques are used. Each strategy's selection is made using q_2 , that needs to be evaluated just before the pursuit process and those values must be within the range of 0 and 1. This phase starts with the creation of r_{q_2} , an arbitrary value from 0 to 1. The siege-fight strategy is employed progressively even if the value is larger than or equal to the q_2 factor. The rotating flight method is used, nevertheless, if this randomized number is less than the value of q_2 and is given in (38).

$$q(i+1) = \begin{cases} Eqn(39) & \text{if } q_2 \geq r_{q_2} \\ Eqn(43) & \text{if } q_2 < r_{q_2} \end{cases} \quad (38)$$

Conflict over food:

When numerous vultures congregate in a single food supply, they can create violent conflicts among food. Powerful vultures stay away from less strong vultures throughout such instances. If not, the weaker vultures will flock towards the stronger vultures and initiate small battles with them to burn them out and grab their food:

$$q(i+1) = d(i) \times (S + r_4) - D(t) \quad (39)$$

$$D(t) = H(i) - q(i) \quad (40)$$

$$d(i) = |X \times H(i) - q(i)| \quad (41)$$

Here, r_4 signifies the randomized count among 0 and 1 that raises the randomness factor. Among the two different pairs of vultures, $H(i)$ was selected as one of the optimal vultures. The vulture's current vector location is indicated by $q(i)$. This equation provides the separation among vultures, one of the most prominent vultures of both groups. $X = 2r$ is a quantity vector to enhance the randomized action, which varies with every iteration.

Vultures' ability to rotate:

Spiral motion is used in this stage to mimic rotating motion. With this approach, a spiral calculation is established among each vulture and is considered as one of the two most vultures. Thus, the rotating flight expression is given in (42) and (43).

$$V_1 = H(i) \times \left(\frac{r_5 \times q(i)}{2\pi} \right) \times \cos(q(i))$$

$$V_2 = H(i) \times \left(\frac{r_6 \times q(i)}{2\pi} \right) \times \sin(q(i)) \tag{42}$$

$$q(i + 1) = H(i) - (V_1 + V_2) \tag{43}$$

Stage 2:

All vulture's movements regarding the food supply are evaluated at this stage. The q_3 variable is defined in (44) to calculate the selecting rate for every method; while r_{q3} is an arbitrary count among zero and one.

$$q(i + 1) = \begin{cases} Eqn(47)if & q_3 \geq r_{q3} \\ Eqn(48)if & q_3 < r_{q3} \end{cases} \tag{44}$$

Various vulture groups congregated at their food source:

The direction of each vulture's flight towards the food source is watched. When there is a strong battle for food and vultures are starving, several groups of vultures might congregate in a single food source. Here, AO uses the target's chosen location for its benefit to approach and attack the victim:

$$A_1 = (Bestvulture_1(i) - X_m * \alpha - r + (u_b - l_b) * r + l_b) * \beta \tag{45}$$

$$A_2 = (Bestvulture_2(i) - X_m * \alpha - r + (u_b - l_b) * r + l_b) * \beta \tag{46}$$

While, α and β implies the exploited alteration constraints with a low value of 0 and 1. $Bestvulture_1(i)$ and $Bestvulture_2(i)$ represents the top vultures in the first and second group of the present iteration:

$$q(i + 1) = \frac{A_1 + A_2}{2} \tag{47}$$

In the end, all vultures are aggregated using (47), where A_1 and A_2 are determined employing (45) and (46), where $q(i + 1)$ signifies the vector representing the vulture spot in the subsequent iteration.

Fighting for food aggressively:

The primary vultures are feeling weak and starving at this stage, but they are also becoming hostile. Moreover, it should also approach the leading vulture from different angles. This movement was modelled using (48).

$$q(i + 1) = H(i) - |D(t)| \times S \times L(d) \tag{48}$$

The EA-AVO technique in (48) has been made more effective by utilizing the levy flight function's flight patterns. Algorithm 1 exposes the pseudocode of the developed EA-AVO approach. Figure 2 depicts the flow diagram of the created EA-AVO technique.

Algorithm 1. Pseudocode of EA-AVO approach

```
Pseudocode of EA-AVO Approach
Prepare the randomized populace  $q_i$ 
While (the stop condition is not met) do
    Calculate the fitness of the vulture
    Set  $bestvulture_1$  as the top best vulture spot
```

```

Set bestvulture2 as the next ideal vulture position
for (every qivulture) do
    Using 32) select H(i)
    Using (34) update the S
    if (|S| ≥ 1) then
        if (q1 ≥ rq1) then
            The position of the vulture is updated in (35)
        else
            (37) will be upgraded
    if (|S| < 1) then
        if (|S| ≥ 0.5) then
            if (q2 ≥ rq2) then
                The position of the vulture is updated in (39)
            else
                (43) will be upgraded
        else
            if (q3 ≥ rq3) then
                The position of the vulture is updated in (47)
            else
                (48) will be upgraded
Return the best vulture
    
```

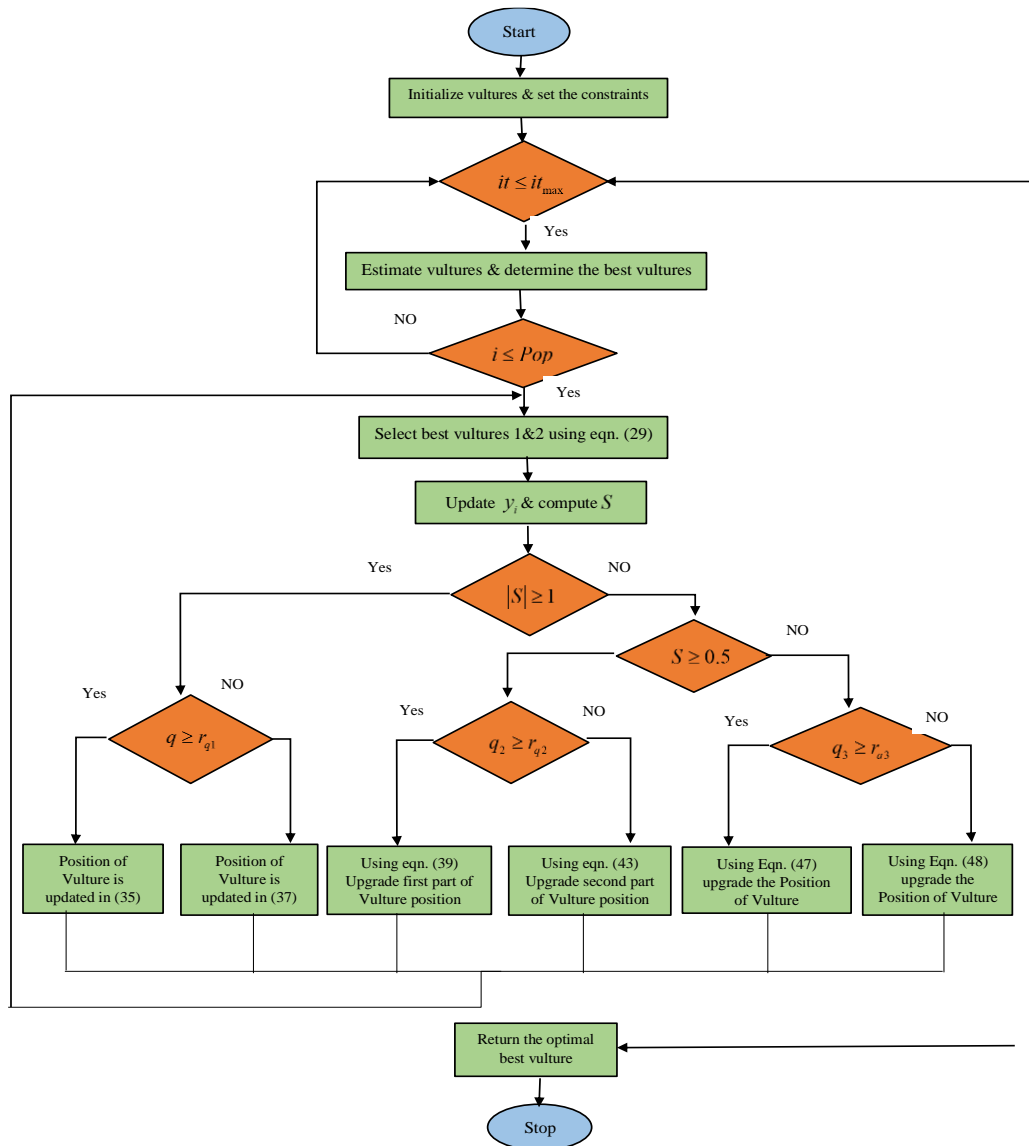


Figure 2. Flowchart of proposed EA-AVO approach

5. RESULTS AND DISCUSSION

5.1. Simulation setup

In MATLAB 2021b, simulations were run for the suggested model to control PMSG-based wind power generation using a hybrid EA-AVO approach. The stability and dynamic performances of the WTG system are shown in this part to exemplify the potency of the suggested controlling approach. Regarding copper loss, Core loss and Total loss, the performance of the preferred model was compared to other widely used techniques including AQO [35], AVOA [34], GOA [36], and WHO+PI [22]. Table 2 design parameters.

Table 2. design parameters

Parameters	Values
Blade pitch angle	Beta = 35
Rotor speed	wg = 1200/60
Wind speed	Vw = 10
Constant	Kw = 0.1
Rs	0.1764
Kr	0.2083/60
Ld	6.24*10 ⁻³
Lq	20.5822*10 ⁻³
sim	0.246

5.2. Performance findings with regard to losses

Table 3 depicts the outcomes in terms of copper loss, which demonstrates that the suggested model is superior to other approaches almost at all rotor speeds. The rotor speed is raised in this instance from 50 to 1000 in ascending sequence. The suggested approach gives minimum copper loss when compared to the standard techniques at any speed. The results of the core loss for both the presented and traditional strategies are summarised in Table 4. Table 3 core loss demonstrates that even when the speed of the rotor increases, the core loss of the suggested framework is significantly lower than that of standard approaches. In particular, at rotor speed 500 rpm, the suggested scheme acquired less core loss of 95.181, which is superior to AQO, AVOA, GOA, and WHO+PI. This outcome supports the importance of the suggested work. The betterment is due to the deployment of a hybrid EA-AVO algorithm that combines the concepts of AOA and AVOA, which helps in optimally handling the polynomial restrictions to maximize wind energy output by minimizing IPMSG losses.

The total loss, also known as the aggregate loss, is summarised in Table 5. Both core and copper losses are included in the total loss. The total loss at a single speed of the rotor has been summarised in the table, while the novel approach outperforms the standard ones. We found that the suggested approach achieves a lower total loss of 149.62 at the starting stage of 50 rotor speed, and it is 36.46% better than AQO, 36.17% better than AVOA, 36.59% better than GOA approaches, 36.42%, and better than WHO+PI approaches. The proposed method in this study tended to have an inordinately higher proportion of 149.63 for 1000 rotor speed which is 36.38%, 0.16%, 38.39%, and 36.38% better when compared to the suggested model to other current approaches like AQO, AVOA, GOA, and WHO+PI.

Table 3. Performance of proposed control schemes in terms of copper loss

Rotor speed	AQO	AVOA	GOA	WHO+PI [22]	PROP
50	0.000141	0.001152	0.00116	8.34E-05	54.434
100	0.000202	41.11	0.00014	0.00013462	54.434
150	0.000414	0.000292	0.00029	20.146	54.429
200	0.000535	57.039	0.00051	0.00050819	54.435
250	0.001859	51.37	0.00078	0.00077401	54.435
300	0.000715	39.62	0.00108	0.0010815	54.436
350	0.002291	50.522	0.00142	0.0014229	54.435
400	0.001745	53.748	0.00179	0.0017894	54.437
450	0.003016	54.693	0.00217	0.002174	54.437
500	0.002746	34.816	0.00257	0.0025694	54.439
550	0.004132	0.72421	0.00297	0.0029692	54.439
600	0.003608	74.546	0.00337	0.0033689	54.431
650	0.005936	37.365	0.00376	0.0037634	54.442
700	0.004566	64.423	0.00415	0.0041499	54.443
750	0.005318	51.527	0.00453	0.0045252	54.443
800	0.005635	51.401	0.00489	0.0048874	54.444
850	0.004225	2.8607	0.00524	0.0052352	54.44
900	0.009303	57.029	0.00557	0.0055672	54.445
950	0.005729	48.872	0.00588	0.0058833	54.447
1,000	0.009928	49.882	0.00618	0.0061829	54.448

Table 4. Performance of proposed scheme in terms of core loss

Rotor speed	AQO	AVOA	GOA	WHO+PI [22]	PROP
50	235.51	234.4	235.96	235.34	95.182
100	235.24	109.99	235.24	235.22	95.183
150	235.21	235.18	235.21	316.36	95.187
200	235.19	92.631	235.23	235.19	95.182
250	235.23	98.319	235.21	235.19	95.183
300	235.19	112.21	235.2	235.19	95.182
350	235.2	99.252	235.2	235.19	95.184
400	235.19	95.898	235.2	235.19	95.182
450	235.19	94.931	235.2	235.19	95.183
500	235.19	118.34	235.2	235.19	95.181
550	235.2	215.93	235.19	235.19	95.182
600	235.2	77.973	235.2	235.2	95.191
650	235.2	115.52	235.2	235.2	95.181
700	235.2	85.861	235.2	235.2	95.181
750	235.2	98.164	235.2	235.2	95.181
800	235.2	98.301	235.2	235.2	95.181
850	235.21	197.94	235.21	235.2	95.186
900	235.21	92.649	235.21	235.21	95.182
950	235.21	102.66	235.21	235.21	95.181
1,000	235.22	99.993	235.21	235.21	95.181

Table 5. Performance of the current scheme in terms of overall loss

Rotor speed	AQO	AVOA	GOA	WHO+PI [22]	PROP
50	235.51	234.41	235.96	235.34	149.62
100	235.24	151.1	235.24	235.22	149.62
150	235.21	235.18	235.21	336.51	149.62
200	235.19	149.67	235.23	235.19	149.62
250	235.23	149.69	235.21	235.19	149.62
300	235.19	151.83	235.2	235.19	149.62
350	235.2	149.77	235.2	235.19	149.62
400	235.19	149.65	235.2	235.19	149.62
450	235.2	149.62	235.2	235.19	149.62
500	235.19	153.16	235.2	235.19	149.62
550	235.2	216.65	235.2	235.2	149.62
600	235.2	152.52	235.2	235.2	149.62
650	235.21	152.88	235.2	235.2	149.62
700	235.2	150.28	235.2	235.2	149.62
750	235.21	149.69	235.21	235.21	149.62
800	235.21	149.7	235.21	235.21	149.63
850	235.21	200.8	235.21	235.21	149.63
900	235.22	149.68	235.21	235.21	149.63
950	235.21	151.54	235.22	235.21	149.63
1,000	235.23	149.88	235.22	235.22	149.63

5.3. Input and output power

A permanent magnet synchronous motor (PMSM) is an AC electric motor that uses magnetic interaction to transform electrical energy into mechanical energy. This section discusses the mechanical input and electrical output power of the IPMSG for different rotor speeds. Table 6 provides a summary of the projected EA-AVO model's mechanical inputs as well as electrical output power. From Table 6 it can be that when the rotor speed is 500 rpm the electrical output power attained by the proposed EA-AVO method is -1.3388(W). Likewise, at rotor speed 1000, the mechanical input power is -2.6799 and the electrical output power is -2.6788.

5.4. Ideal value of I_q 's speed of the rotor

To enhance wind power generation the quadrature axis current I_q is optimized using the proposed EA-AVO method. The graphic assessment in Figure 3 examines the effectiveness of the suggested scheme along with different techniques for achieving ideal values of $I_{q,opt}$ against IPMSG rotational speed. The graphs are displayed with rotor speeds ranging from 0 to 1,200. It is clear from Figure 3 that the ideal values of the novel EA-AVO strategy provide a superior optimal solution when compared to other conventional methods like AQO, AVOA, GOA, and WHO+PI.

Table 6. Input/output power of proposed EA-AVO

Rotor speed	Mechanical input power	Electrical output power
50	-0.13386	-0.13277
100	-0.26795	-0.26795
150	-0.40195	-0.40078
200	-0.53595	-0.53479
250	-0.66995	-0.66876
300	-0.80389	-0.80272
350	-0.93795	-0.93674
400	-1.0719	-1.0706
450	-1.2059	-1.2048
500	-1.3399	-1.3388
550	-1.4739	-1.4727
600	-1.6079	-1.6068
650	-1.7419	-1.7407
700	-1.8759	-1.8748
750	-2.0099	-2.0085
800	-2.1439	-2.1427
850	-2.2779	-2.2768
900	-2.4119	-2.4111
950	-2.5459	-2.5448
1000	-2.6799	-2.6788

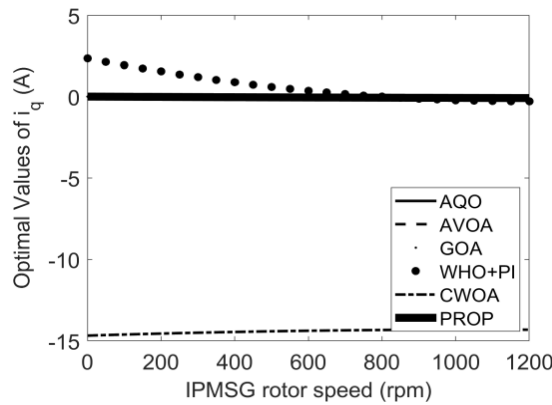


Figure 3. Achieved ideal value of $I_{q,opt}$

5.5. Convergence analysis

By altering the number of iterations from 0 to 100, Figure 4 illustrates the cost function assessment of the offered technique. It is clear from the graph that the created model successfully lowers the loss when compared to other prevailing schemes. Initially, the cost function of the suggested system is 401.67, which is 60.08%, 7.93%, 22.92%, and 76.88% better than the AQO, AVOA, GOA, and WHO+PI strategies. Nevertheless, the cost function of the suggested model decreases as the number of iterations rises, and is seen from the curve given in the graph. According to Figure 4, the selected approach achieved a quick convergence of 148.03 better than AQO, AVOA, GOA, and WHO+PI, respectively, for the 80th iteration with a minimised cost function. The suggested model also achieved a quick convergence at iteration 100, equal to 148.03, which is better than AQO, AVOA, GOA and WHO+PI by 37.13%, 1.05%, 71.15%, and 37.12% respectively. Our study suggests that AI-AVO’s method is superior to other standard approaches with a minimized cost function. The proposed method may benefit from the conceptual incorporation of prevailing techniques, like the aquila optimization algorithm (AOA) and the AVO algorithm without adversely impacting the parameter setting.

5.6. Optimization efficiency

The line graph in Figure 5 proves the suggested strategy’s effectiveness. This has been demonstrated by distinguishing between concepts such as, with and without optimization. The efficacy rating has been established in percent for all rotor speeds. There is no doubt that the offered technique with optimisation has produced better outcomes and higher efficacy. Instantly, while the rotor running at 50 rpm, the developed design with an optimization approach has improved effectiveness to a level of 98.7%, as well as the curve

rises slowly as it approaches the highest speed of 1,000 Nm. As shown in Figure 5, the suggested model with optimization has demonstrated greater efficiency in comparison to the proposed model without optimisation.

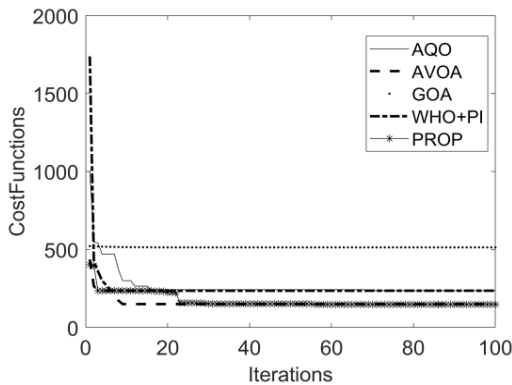


Figure 4. Convergence graph of preferred AI-AVO approach

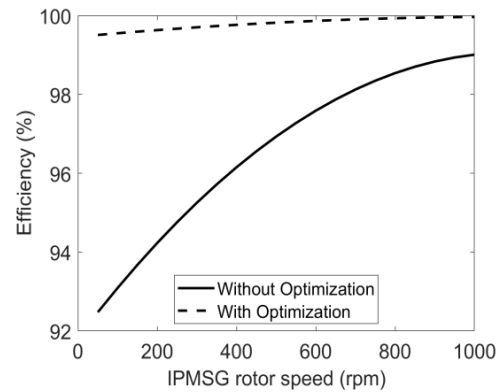


Figure 5. Optimization efficiency performance

6. DISCUSSION

This study explored a comprehensive optimization strategy for the highest wind power generation with a reduced overall loss in PMSG-based WECS. Here, the results of the proposed model have been compared with existing models like AQO [35], AVOA [34], GOA [36], and WHO+PI [22] concerning the copper loss, core loss and total loss. The analysis based on losses reveals that that the suggested method attains a lower total loss of at the starting stage of 50 rotor speed, and is better than AQO, AVOA, GOA, and WHO+PI approaches. Likewise, the analysis of convergence shows that the proposed method attains quick convergence than the AQO, AVOA, GOA, and WHO+PI. Likewise, the proposed model offers better efficiency when compared with the proposed model without optimisation. This superiority is due to the conceptual incorporation of prevailing techniques, like the AOA and the AVO algorithm. According to the results of this experimental work, the PMSM is the most effective way to simulate the features of wind turbines for use in the study and creation of WECSs. However, further and in-depth studies may be needed to confirm the limitations of this study, especially regarding the nonlinear dynamical system stabilization problem that has not been focused.

7. CONCLUSION

The recent observations suggest that there is a need for an efficient MPPT technique for modern conversion systems. This article suggested a novel optimization strategy for the highest wind power generation with a reduced overall loss in PMSG-based WECS. The TPR, rotor speed ω_g , and quadrature axis current I_q will be optimized in the proposed work to enhance the generated wind energy. Further, the direct axis current I_d will be calculated from the optimized rotor speed ω_g . The optimization will be carried out using the hybrid optimization named AI-AVO algorithm. Regarding core loss, copper loss, and total loss, the effectiveness of the suggested framework has been contrasted to those of various methods already in use, including AQO, AVOA, GOA, and WHO+PI. Additionally, the recommended system's effectiveness was shown. Our findings provide conclusive evidence that the suggested model attains less overall loss of 149.62 at the starting stage of 50 rotor speed, and it was 36.46% better than AQO, 36.17% better than AVOA, 36.59% better than GOA approaches 36.42% and better than WHO+PI approaches. For 1000 rotor speed, it is seen that the current model is 149.63, which is 36.38%, 0.16%, 38.39%, and 36.38% better when compared to the suggested model to other current approaches, like AQO, AVOA, GOA, and WHO+PI individually. Our study demonstrates that the outcomes attained are more resilient than previous studies. The proposed method has overcome the issues in the existing work like low convergence, copper loss, core loss, total loss, and less efficiency. Future studies may explore on the sensorless control scheme for PMSG-based WECS, with feasible ways of producing a sensorless control scheme for PMSG-based WECSs.

REFERENCES

- [1] S. Li, T. A. Haskew, R. P. Swatloski, and W. Gathings, "Optimal and direct-current vector control of direct-driven PMSG wind turbines," *IEEE Transactions on Power Electronics*, vol. 27, no. 5, pp. 2325–2337, May 2012, doi: 10.1109/TPEL.2011.2174254.
- [2] J. Lagorse, M. G. Simoes, and A. Miraoui, "A multiagent fuzzy-logic-based energy management of hybrid systems," *IEEE Transactions on Industry Applications*, vol. 45, no. 6, pp. 2123–2129, 2009, doi: 10.1109/TIA.2009.2031786.
- [3] X. Tan, Q. Li, and H. Wang, "Advances and trends of energy storage technology in Microgrid," *International Journal of Electrical Power and Energy Systems*, vol. 44, no. 1, pp. 179–191, Jan. 2013, doi: 10.1016/j.ijepes.2012.07.015.
- [4] P. F. Ribeiro, B. K. Johnson, M. L. Crow, A. Arsoy, and Y. Liu, "Energy storage systems for advances power applications," *Proceedings of the IEEE*, vol. 89, no. 12, pp. 1744–1756, 2001, doi: 10.1109/5.975900.
- [5] A. Chauhan and R. P. Saini, "A review on integrated renewable energy system based power generation for stand-alone applications: configurations, storage options, sizing methodologies and control," *Renewable and Sustainable Energy Reviews*, vol. 38, pp. 99–120, Oct. 2014, doi: 10.1016/j.rser.2014.05.079.
- [6] C. N. Bhende, S. Mishra, and S. G. Malla, "Permanent magnet synchronous generator-based standalone wind energy supply system," *IEEE Transactions on Sustainable Energy*, vol. 2, no. 4, pp. 361–373, Oct. 2011, doi: 10.1109/TSTE.2011.2159253.
- [7] Y. Chen, P. Pillay, and A. Khan, "PM wind generator topologies," *IEEE Transactions on Industry Applications*, vol. 41, no. 6, pp. 1619–1626, Nov. 2005, doi: 10.1109/TIA.2005.858261.
- [8] F. Valenciaga and P. F. Puleston, "High-order sliding control for a wind energy conversion system based on a permanent magnet synchronous generator," *IEEE Transactions on Energy Conversion*, vol. 23, no. 3, pp. 860–867, Sep. 2008, doi: 10.1109/TEC.2008.922013.
- [9] S. Grabic, N. Celanovic, and V. A. Katic, "Permanent magnet synchronous generator cascade for wind turbine application," *IEEE Transactions on Power Electronics*, vol. 23, no. 3, pp. 1136–1142, May 2008, doi: 10.1109/TPEL.2008.921181.
- [10] C. Mademlis and N. Margaris, "Loss minimization in vector-controlled interior permanent-magnet synchronous motor drives," *IEEE Transactions on Industrial Electronics*, vol. 49, no. 6, pp. 1344–1347, Dec. 2002, doi: 10.1109/TIE.2002.804990.
- [11] C. Cavallaro, A. O. Di Tommaso, R. Miceli, A. Raciti, G. R. Galluzzo, and M. Trapanese, "Efficiency enhancement of permanent-magnet synchronous motor drives by online loss minimization approaches," *IEEE Transactions on Industrial Electronics*, vol. 52, no. 4, pp. 1153–1160, Aug. 2005, doi: 10.1109/TIE.2005.851595.
- [12] Q. Zhu, Ed., *Nonlinear Systems*. MDPI, 2023.
- [13] K. Palanimuthu, G. Mayilsamy, S. R. Lee, S. Y. Jung, and Y. H. Joo, "Comparative analysis of maximum power extraction and control methods between PMSG and PMVG-based wind turbine systems," *International Journal of Electrical Power & Energy Systems*, vol. 143, p. 108475, Dec. 2022, doi: 10.1016/j.ijepes.2022.108475.
- [14] M. K. K. Prince, M. T. Arif, A. Gargoom, A. M. T. Oo, and M. E. Haque, "Modeling, parameter measurement, and control of PMSG-based grid-connected wind energy conversion system," *Journal of Modern Power Systems and Clean Energy*, vol. 9, no. 5, pp. 1054–1065, 2021, doi: 10.35833/MPCE.2020.000601.
- [15] B. Majout *et al.*, "Improvement of PMSG-based wind energy conversion system using developed sliding mode control," *Energies*, vol. 15, no. 5, p. 1625, Feb. 2022, doi: 10.3390/en15051625.
- [16] M. Chinchilla, S. Arnaltes, and J. C. Burgos, "Control of permanent-magnet generators applied to variable-speed wind-energy systems connected to the grid," *IEEE Transactions on Energy Conversion*, vol. 21, no. 1, pp. 130–135, Mar. 2006, doi: 10.1109/TEC.2005.853735.
- [17] C. Mademlis and V. G. Agelidis, "On considering magnetic saturation with maximum torque to current control in interior permanent magnet synchronous motor drives," *IEEE Transactions on Energy Conversion*, vol. 16, no. 3, pp. 246–252, 2001, doi: 10.1109/60.937204.
- [18] Ö. Çelik and A. Teke, "A hybrid MPPT method for grid connected photovoltaic systems under rapidly changing atmospheric conditions," *Electric Power Systems Research*, vol. 152, pp. 194–210, Nov. 2017, doi: 10.1016/j.epsr.2017.07.011.
- [19] S. Li, H. Wang, Y. Tian, and A. Aitouche, "A RBF neural network based MPPT method for variable speed wind turbine system," *IFAC-PapersOnLine*, vol. 28, no. 21, pp. 244–250, 2015, doi: 10.1016/j.ifacol.2015.09.535.
- [20] M. A. Rahman, D. M. Vilathgamuwa, M. N. Uddin, and K. J. Tseng, "Nonlinear control of interior permanent-magnet synchronous motor," *IEEE Transactions on Industry Applications*, vol. 39, no. 2, pp. 408–416, Mar. 2003, doi: 10.1109/TIA.2003.808932.
- [21] P. S. Chinamalli and M. Sasikala, "CWOA-PMSG: crossover assisted WOA optimization for controlling PMSG in wind generation system," in *3rd International Conference on Electrical, Electronics, Communication, Computer Technologies and Optimization Techniques, ICEECCOT 2018*, Dec. 2018, pp. 654–664, doi: 10.1109/ICEECCOT43722.2018.9001403.
- [22] M. M. Mahmoud, "Improved current control loops in wind side converter with the support of wild horse optimizer for enhancing the dynamic performance of PMSG-based wind generation system," *International Journal of Modelling and Simulation*, vol. 43, no. 6, pp. 952–966, Nov. 2023, doi: 10.1080/02286203.2022.2139128.
- [23] L. Shanmugam and Y. H. Joo, "Stabilization of permanent magnet synchronous generator-based wind turbine system via fuzzy-based sampled-data control approach," *Information Sciences*, vol. 559, pp. 270–285, Jun. 2021, doi: 10.1016/j.ins.2020.12.088.
- [24] E. H. Dursun, H. Koyuncu, and A. A. Kulaksiz, "A novel unified maximum power extraction framework for PMSG based WECS using chaotic particle swarm optimization derivatives," *Engineering Science and Technology, an International Journal*, vol. 24, no. 1, pp. 158–170, Feb. 2021, doi: 10.1016/j.jestch.2020.05.005.
- [25] S. A. Hussien, M. A. Deab, and F. Alrowais, "Maximization of the power delivered from permanent magnet synchronous generator wind energy conversion system to the grid based on using moth flame optimization," *Indonesian Journal of Electrical Engineering and Computer Science*, vol. 27, no. 3, pp. 1347–1357, Sep. 2022, doi: 10.11591/ijeecs.v27.i3.pp1347-1357.
- [26] A. Fathy, A. G. Alharbi, S. Alshammari, and H. M. Hasanien, "Archimedes optimization algorithm based maximum power point tracker for wind energy generation system," *Ain Shams Engineering Journal*, vol. 13, no. 2, p. 101548, Mar. 2022, doi: 10.1016/j.asej.2021.06.032.
- [27] M. M. Mahmoud, M. M. Aly, and A. M. M. Abdel-Rahim, "Enhancing the dynamic performance of a wind-driven PMSG implementing different optimization techniques," *SN Applied Sciences*, vol. 2, no. 4, 2020, doi: 10.1007/s42452-020-2439-3.
- [28] W. Qiao, L. Qu, and R. G. Harley, "Control of IPM synchronous generator for maximum wind power generation considering magnetic saturation," *IEEE Transactions on Industry Applications*, vol. 45, no. 3, pp. 1095–1105, 2009, doi: 10.1109/TIA.2009.2018914.
- [29] P. M. Anderson and A. Bose, "Stability simulation of wind turbine systems," *IEEE Transactions on Power Apparatus and Systems*, vol. PAS-102, no. 12, pp. 3791–3795, Dec. 1983, doi: 10.1109/TPAS.1983.317873.

- [30] S. Morimoto, M. Sanada, and Y. Takeda, "Effects and compensation of magnetic saturation in flux-weakening controlled permanent magnet synchronous motor drives," *IEEE Transactions on Industry Applications*, vol. 30, no. 6, pp. 1632–1637, Nov. 1994, doi: 10.1109/TIA.1994.350318.
- [31] S. Morimoto, H. Nakayama, M. Sanada, and Y. Takeda, "Sensorless output maximization control for variable-speed wind generation system using IPMSG," *IEEE Transactions on Industry Applications*, vol. 41, no. 1, pp. 60–67, Jan. 2005, doi: 10.1109/TIA.2004.841159.
- [32] N. Urasaki, T. Senjyu, and K. Uezato, "A novel calculation method for iron loss resistance suitable in modeling permanent-magnet synchronous motors," *IEEE Transactions on Energy Conversion*, vol. 18, no. 1, pp. 41–47, Mar. 2003, doi: 10.1109/TEC.2002.808329.
- [33] J. Y. Seol and I. J. Ha, "Feedback-linearizing control of IPM motors considering magnetic saturation effect," *IEEE Transactions on Power Electronics*, vol. 20, no. 2, pp. 416–424, Mar. 2005, doi: 10.1109/TPEL.2004.842980.
- [34] B. Abdollahzadeh, F. S. Gharehchopogh, and S. Mirjalili, "African vultures optimization algorithm: a new nature-inspired metaheuristic algorithm for global optimization problems," *Computers & Industrial Engineering*, vol. 158, p. 107408, Aug. 2021, doi: 10.1016/j.cie.2021.107408.
- [35] L. Abualigah, D. Yousri, M. A. Elaziz, A. A. Ewees, M. A. A. Al-qaness, and A. H. Gandomi, "Aquila optimizer: a novel metaheuristic optimization algorithm," *Computers and Industrial Engineering*, vol. 157, p. 107250, Jul. 2021, doi: 10.1016/j.cie.2021.107250.
- [36] Y. Meraihi, A. B. Gabis, S. Mirjalili, and A. Ramdane-Cherif, "Grasshopper optimization algorithm: theory, variants, and applications," *IEEE Access*, vol. 9, pp. 50001–50024, 2021, doi: 10.1109/ACCESS.2021.3067597.

BIOGRAPHIES OF AUTHORS



Prashant Kumar S. Chinamalli    born on 10th June 1987, received his B.E. degree in Electrical and Electronics Engineering department from Poojya Doddappa Appa Engineering College, Gulbarga in 2010. M.Tech. in Power and Energy System from Basaveshwara Engineering College, Bagalkot in 2012. He is working as Assistant Professor at Department of Electrical and Electronics Engineering, Faculty of Engineering and Technology (Co-Ed), Sharnbasva University, Kalaburagi, with an experience of 11 years. His areas of interest include power system, drives and renewable energy sources. He can be contacted at email: prashantvnc@gmail.com.



Dr. Mungamuri Sasikala    born on 10th December 1962, received her B.E. degree in Electrical and Engineering and M.E. in Power Systems from Osmania University, Hyderabad. She is Currently working as Professorate Department of Electrical and Electronics Engineering, Faculty of Engineering and Technology for Women, Sharnbasva University, Kalaburagi with an experience of 25 years. Her areas of interest include fuzzy logic, sensors, power system, power electronics and drives. She can be contacted at email: sasi_mun@rediffmail.com.